

# 1 Grey and white matter micro-structure is associated 2 with polygenic risk for schizophrenia

3 Eva-Maria Stauffer<sup>1,\*</sup>, Richard A.I. Bethlehem<sup>1,†</sup>, Varun Warriar<sup>1,†</sup>, Graham K. Murray<sup>1,2,3</sup>,  
4 Rafael Romero-Garcia<sup>1</sup>, Jakob Seidlitz<sup>4,5</sup>, and Edward T. Bullmore<sup>1</sup>

5 <sup>1</sup>University of Cambridge, Department of Psychiatry, Cambridge Biomedical Campus, CB2 0SZ, UK

6 <sup>2</sup>Cambridgeshire and Peterborough NHS Trust, Elizabeth House, Fulbourn Hospital, Cambridge CB21 5EE, UK

7 <sup>3</sup>Institute for Molecular Bioscience, University of Queensland, St Lucia 4072, Australia

8 <sup>4</sup>Department of Child and Adolescent Psychiatry and Behavioral Science, Children's Hospital of Philadelphia, Philadelphia, PA, USA

9 <sup>5</sup>Department of Psychiatry, University of Pennsylvania, Philadelphia, PA, USA

10 \*corresponding author(s): Eva-Maria Stauffer (ems206@cam.ac.uk)

11 †these authors contributed equally to this work

## 13 ABSTRACT

### Background

Recent discovery of approximately 270 common genetic variants associated with schizophrenia has enabled polygenic risk scores (PRS) to be measured in the population. We hypothesized that normal variation in PRS would be associated with magnetic resonance imaging (MRI) phenotypes of brain morphometry and tissue composition.

### Methods

We used the largest extant genome-wide association dataset (N = 69,369 cases and N = 236,642 healthy controls) to measure PRS for schizophrenia in a large sample of adults from the UK Biobank (N<sub>max</sub> = 29,878) who had multiple micro- and macro-structural MRI metrics measured at each of 180 cortical areas, seven subcortical structures, and 15 major white matter tracts. Linear mixed effect models were used to investigate associations between PRS and brain structure at global and regional scales, controlled for multiple comparisons.

### 14 Results

Polygenic risk was significantly associated with reduced neurite density index (NDI) at global brain scale, at 149 cortical regions, five subcortical structures and 14 white matter tracts. Other micro-structural parameters, e.g., fractional anisotropy, that were correlated with NDI were also significantly associated with PRS. Genetic effects on multiple MRI phenotypes were co-located in temporal, cingulate and prefrontal cortical areas, insula, and hippocampus. Post-hoc bidirectional Mendelian randomization analyses provided preliminary evidence in support of a causal relationship between (reduced) thalamic NDI and (increased) risk of schizophrenia.

### Conclusions

Risk-related reduction in NDI is plausibly indicative of reduced density of myelinated axons and dendritic arborization in large-scale cortico-subcortical networks. Cortical, subcortical and white matter micro-structure may be linked to the genetic mechanisms of schizophrenia.

### Keywords

NODDI, DWI, false discovery rate, GWAS, PheWAS, UK Biobank

## 15 Introduction

16 A substantial genetic contribution to the pathogenesis of schizophrenia is indicated by twin and familial heritability estimates of  
17 approximately 80% [1, 2, 3], and SNP heritability of approximately 24% [4]. The most recent genome-wide association study  
18 (GWAS) identified 270 risk-associated loci, allowing the construction of polygenic risk scores (PRS) that explain up to 7.7% of  
19 the variance in schizophrenia [4]. Polygenic risk scores are normally distributed in the general population and have been used  
20 to investigate the shared genetics between schizophrenia, neurodevelopmental trajectories and brain morphology [5, 6].

21 The genetic liability for schizophrenia is thought to cause proximal changes in brain structure and function [7], which  
22 then result in distal changes in psychological function and clinical symptoms characteristic of schizophrenia [8, 9, 10, 11].  
23 Although brain structural abnormalities have been consistently reported in schizophrenia case-control studies [12, 13, 14],  
24 and are substantially heritable [15, 16, 17], the current evidence linking magnetic resonance imaging (MRI) markers of brain  
25 structure to polygenic risk for schizophrenia is inconsistent [18]. Recent studies reported no significant associations between  
26 PRS and volume of subcortical nuclei [19, 20, 21], or between PRS and white matter structure [19]. Some studies have reported  
27 significant negative associations between PRS and global brain measures, such as total white matter volume (WMV) [22]) or  
28 mean cortical thickness (CT) [6]; but effect sizes have been small ( $R^2 = 0.2\%$ ) and not consistently significant between studies  
29 [18, 19]. Thickness of insular cortex was specifically associated with polygenic risk for schizophrenia ( $R^2 = 0.2\%$ ) [6] but most  
30 prior studies have not found significant associations between PRS and regional brain anatomy [18].

31 The current lack of clear evidence for an association between genetic risk for schizophrenia and brain structure could be  
32 attributable to the relatively small sample sizes of prior genetic neuroimaging studies ( $100 < N < 15,000$ ), which were likely  
33 under-powered to detect small polygenic effects [6, 18, 19, 21]. Inherently low power is necessarily exacerbated when type I  
34 error is appropriately adjusted to control for multiple testing of regional phenotypes [6]. It is also notable that cortical and  
35 subcortical MRI phenotypes so far investigated have mostly been macro-structural metrics, e.g., cortical thickness, which are  
36 coarse-grained compared to the predicted effects of risk genes on tissue composition and cellular organization.

37 Case-control studies of schizophrenia have consistently reported significant reductions in regional cortical thickness (CT),  
38 surface area (SA) [13], grey matter volume (Vol)[23], intrinsic curvature (IC, a metric of local connectivity of cortex) [24] and  
39 local gyrification index (LGI, a metric of cortical folding) [25]. These are all macro-structural markers of brain morphology that  
40 are derived from T1-weighted MRI data and estimated each cortical or subcortical region. In contrast, micro-structural MRI  
41 phenotypes are derived from diffusion-weighted imaging (DWI) data, providing finer-grained information about the cellular  
42 composition of brain tissue [26, 27, 28]. Case-control studies of schizophrenia have increasingly reported significant differences  
43 in grey matter micro-structure (26), such as increased mean diffusivity (MD) [28, 29, 30], decreased fractional anisotropy (FA)  
44 [31], decreased neurite density index (NDI) [26] and orientation dispersion index (ODI) [32]. Significant micro-structural  
45 abnormalities of white matter tracts have also been reported, including decreased FA [14, 33] and NDI [34, 35], and increased  
46 MD [14], in schizophrenia case-control studies.

47 We therefore hypothesized that macro- and micro-structural MRI markers of grey and white matter would be associated  
48 with polygenic risk for schizophrenia. We analysed multimodal MRI and genotype data from  $N \sim 30,000$  participants in the  
49 UK Biobank to conduct a comprehensive study of PRS association with nine brain MRI phenotypes (Fig.1). In grey matter, we  
50 measured five macro-structural (CT, SA, Vol, LGI and IC) and four micro-structural (FA, MD, NDI and ODI) MRI metrics in  
51 180 bilateral cortical areas; and a subset of these metrics (Vol, FA, MD, NDI and ODI) in 7 subcortical regions. In white matter,  
52 we measured FA, MD, NDI and ODI in 15 major axonal tracts. We used the largest available GWAS dataset for schizophrenia  
53 ( $N = 69,369$  cases and  $N = 236,642$  controls) to construct schizophrenia PRS for each subject [4]. We expected that this  
54 combination of increased sample size for PRS estimation, and MRI measurement of both macro- and micro-structural metrics,  
55 would enhance statistical power to test the hypothesis that MRI phenotypes are associated with schizophrenia PRS in the  
56 population. In light of the significant associations we discovered by these analyses, we were stimulated to conduct post-hoc  
57 analyses of the causal relationships between a subset of NDI metrics and schizophrenia, using Mendelian randomization and  
58 genetic correlations.

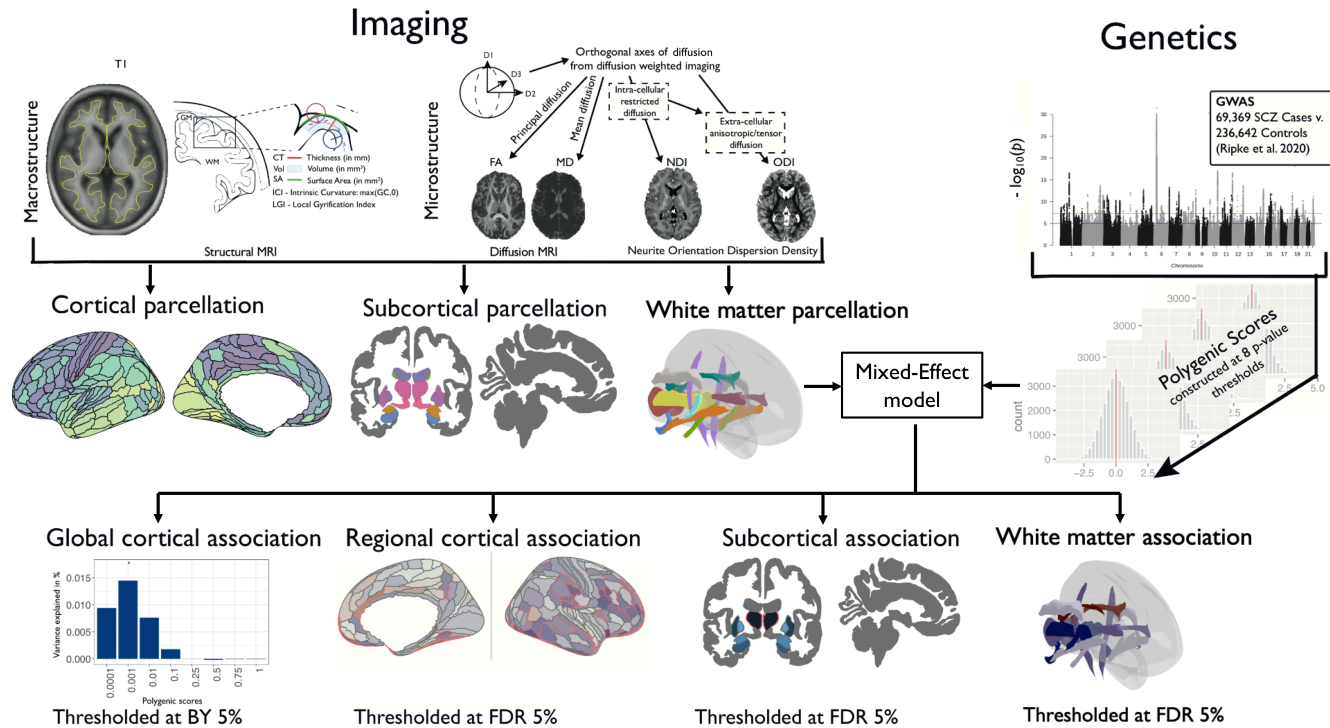


**Figure 1. Schematic summary of the study.** We estimated five macro-structural metrics and four micro-structural metrics at each of 180 bilateral cortical areas, and on average over all cortical areas, for variable numbers of subjects in the UK Biobank for whom quality-controlled data were available: for cortical thickness (CT),  $N = 29,778$ ; surface area (SA),  $N = 29,777$ ; grey matter volume (Vol),  $N = 29,778$ ; intrinsic curvature (IC),  $N = 29,676$ ; local gyriification index (LGI),  $N = 27,086$ ; fractional anisotropy (FA),  $N = 28,232$ ; mean diffusivity (MD),  $N = 28,165$ ; neurite density index (NDI),  $N = 27,632$ ; and orientation dispersion index (ODI),  $N = 27,658$ . We also estimated one macro-structural metric and four micro-structural metrics at each of seven subcortical regions (amygdala, accumbens, caudate, putamen, pallidum, hippocampus, and thalamus): Vol,  $N = 29,854 - 29,878$ ; FA,  $N = 28,192 - 28,238$ ; MD,  $N = 27,664 - 28,154$ ; NDI,  $N = 27,590 - 27,638$ ; and ODI,  $N = 27,600 - 27,658$ . Additionally, we measured four micro-structural metrics at 15 major white matter tracts: FA,  $N = 27,987 - 28,346$ ; MD,  $N = 28,327 - 28,346$ ; NDI,  $N = 28,247 - 28,337$ ; ODI,  $N = 28,219 - 28,346$ . Polygenic risk scores for schizophrenia (PRS) were based on GWAS data from 69,396 cases and 236,642 controls and were calculated for each participant at eight  $P_{SNP}$ -value thresholds for inclusion of significant variants, using the clumping and thresholding approach [36]. To assess associations between multiple schizophrenia polygenic risk scores and cortical phenotypes, we first used mixed effect models to identify which  $P_{SNP}$ -value threshold(s) produced the PRS most strongly associated with each cortical metric at global scale (Benjamini-Yekutieli corrected 5%). We then used mixed effect models to test the association between the globally most predictive PRS for each metric at each cortical area, controlling for multiple comparisons with the false discovery rate (FDR) at 5%. For subcortical structures and white matter tracts, we tested for association between each MRI metric and each of eight polygenic risk scores, with FDR = 5%. The Manhattan plot is for illustrative purposes only and based on a previously published schizophrenia GWAS [37], downloaded from url: <https://www.med.unc.edu/pgc/pgc-workgroups/>.

## 59 **Methods and Materials**

### 60 **Participants**

61 Data were provided by the UK Biobank, a population-based cohort of >500,000 subjects aged between 39 and 73 years [38].  
62 We focused on a subset of  $N = 40,680$  participants for each of whom complete genotype and multimodal MRI data were  
63 available for download (February 2020); **Fig.S2**. We excluded participants with incomplete MRI data, or with a diagnosis  
64 of schizophrenia (self-reported or by ICD-10 criteria). Prior to analysis of each MRI phenotype, we additionally excluded  
65 participants who were robustly defined as outliers by global or regional metrics more than 5 times the median absolute deviation  
66 from the sample median ( $\pm 5$  MAD), see **SI Methods Sample Selection**. Ethical approval was obtained from the Human  
67 Biology Research Ethics Committee, University of Cambridge (Cambridge, UK).

### 68 **Imaging acquisition and preprocessing**

69 MRI data acquisition has been described in detail elsewhere [39]. Minimally processed T1- and T2-FLAIR- weighted MRI data  
70 (and DWI data) were downloaded from UK Biobank (application 20904) <sup>1</sup> and further processed with Freesurfer (v6.0.1) [40]  
71 using the T2-FLAIR weighted images to improve pial surface reconstruction. Pre-processing steps included bias field correction,  
72 registration to stereotaxic space, intensity normalization, skull-stripping, and grey/white matter segmentation; Following  
73 reconstruction, the Human Connectome Project (HCP) parcellation [41] was aligned to each individual image and regional  
74 metrics were estimated for 180 bilateral cortical areas and seven bilateral subcortical structures. DWI data were co-registered  
75 with the T1-aligned parcellation template to estimate FA and MD at each region. Neurite orientation dispersion and density  
76 imaging (NODDI) reconstruction was performed using the AMICO pipeline [42]. Probabilistic tractography was used to  
77 estimate FA, MD, NDI and ODI values at each of 15 major white matter tracts defined using AutoPtx [43]. Documentation and  
78 code for these processing pipelines is available on Github <sup>2</sup>.

### 79 **Genotyping and genetic quality control**

80 Genome-wide genotype data were available for  $N = 488,377$  participants, with DNA acquisition, imputation and quality control  
81 pipelines as described elsewhere [44]. We excluded participants if they were not primarily of white British ancestry based on  
82 genetic ethnic grouping and subjects with excessive genetic heterozygosity, genotyping rate  $\leq 95\%$ , mismatch between reported  
83 and genetic sex, and genetic relatedness  $> 0.25$  between participants [45]. We also excluded single nucleotide polymorphisms  
84 (SNPs) with minor allele frequency  $\leq 0.01$ , that were not in Hardy-Weinberg equilibrium ( $p \leq 1 \times 10^{-6}$ ), variant call rate  $\leq$   
85  $98\%$ , and an imputation quality score  $\leq 0.4$ , resulting in 5,366,036 SNPs.

### 86 **Polygenic risk scores**

87 A PRS is calculated by multiplying the number of risk alleles by the effect size of each allele and summing the products over  
88 all SNPs for each individual [46]. We used the computationally efficient P-value clumping and thresholding method in PRSice  
89 2 [4, 36, 46, 47]. First, SNPs were clumped using the UK Biobank data as a reference panel so that only the most strongly  
90 associated SNP in a region was retained ( $r^2 = 0.1$ , physical distance = 250 kb) [36]. Second, for each participant, we estimated  
91 a set of eight PRS with varying SNP-wise probability thresholds for inclusion ( $0.0001 \leq P_{SNP} \leq 1$ ) to balance signal to noise  
92 ratio [6, 48, 49].

93 We estimated PRS's for  $N = 29,879$  participants, using effect sizes for each allele from a trans-ancestry GWAS with  $N =$   
94  $69,369$  schizophrenia cases and  $N = 236,642$  healthy controls, mostly ( $\sim 80\%$ ) of European ancestry [4]. Previous studies that  
95 used UK Biobank data to test association of MRI markers with polygenic risk estimated PRS from smaller GWAS datasets of  
96 both European and East Asian ancestry [4, 6, 19]. Thus, we estimated eight PRS from the full trans-ancestry GWAS [4] for  
97 each participant and found that scores were normally distributed at all  $P_{SNP}$  inclusion thresholds (**Figure S3, SI Methods**); the  
98 number of SNPs included in the PRS calculation at each probability threshold is reported in **Table S1**.

### 99 **Statistical analysis**

100 Statistical analyses were conducted in R [50]. We used linear mixed effect (LME, “nlme” package version 3.1-144) models  
101 (Equation 1) to estimate the associations between the scaled PRS and each of the scaled MRI phenotypes with covariates  
102 including age,  $age^2$ , sex, genotype batch, 15 genetic principal components (Data-Field 22006), and x, y and z coordinates of  
103 head position in the scanner to control for static-field heterogeneity (Data-Field 25756-25758) [51]. Hemisphere was fitted as a  
104 random effect, resulting in 180 bilateral regions [6, 19, 52], after testing for PRS-by-hemisphere interactions had demonstrated

<sup>1</sup><https://biobank.ctsu.ox.ac.uk/crystal/crystal/docs/brainmri.pdf>

<sup>2</sup><https://github.com/ucam-department-of-psychiatry/UKB>

105 that none were significant at FDR = 5% (Tables S2-S4).

$$\begin{aligned} \text{MRI Phenotype} \sim & \text{PRS} + \text{Age} + \text{Age}^2 + \text{Sex} + \text{Batch} + 15 \text{ PCs} + \\ & \text{x-coordinate} + \text{y-coordinate} + \text{z-coordinate}, \text{ random} \sim 1 \mid \text{Hemisphere} \end{aligned} \quad (1)$$

106 To identify the optimal  $P_{SNP}$  thresholds for PRS construction, and to minimize the multiple testing required for comprehensive brain regional mapping of genetic associations, we decided a priori on a two-step analysis for cortical phenotypes. First, we estimated and tested the association of all eight polygenic risk scores with each MRI metric at a global cortical scale, using the Benjamini-Yekutieli procedure (BY = 5%) to control for multiple tests over all metrics and thresholds. We thus identified the genome-wide probability threshold for PRS inclusion,  $P_{SNP}$ -global, that produced the polygenic risk score most strongly associated with each global cortical metric. Second, we used the PRS defined by  $P_{SNP}$ -global to test for genetic association with the corresponding metric at a regional scale in 180 cortical areas, covarying for total intracranial volume, with false-discovery rate (FDR) = 5%.

114 For analysis of the smaller number of subcortical regions (7 regions), and white matter tracts (15 tracts), we tested for association with all eight PRSs at each region, with FDR = 5%, to control for the multiple tests entailed (56 and 120, respectively).

117 We performed various sensitivity analyses: First, we repeated the regional cortical analysis using the PRS scores at all other  $P_{SNP}$  thresholds and showed that significant associations between PRS and regional MRI phenotypes were largely conserved across  $P_{SNP}$  thresholds (Figure S4-S12). Second, we covaried for the corresponding global metric in the LME model of PRS associations with regional metrics, which revealed a highly correlated pattern for regional cortical associations (Figure S13). Third we repeated cortical analysis using PRS scores from GWAS data in European samples and showed that our findings were not biased by population stratification (Figure S14-16).

123 We report the proportion of explained phenotypic variance by the PRS in percentages ( $R^2$ ) and standardized effect sizes ( $\beta$ ) throughout.

## 125 Bidirectional Mendelian randomization analyses and genetic correlations

126 We conducted exploratory bidirectional Mendelian randomization (MR) analyses for a subset of imaging phenotypes using the ‘twosampleMR’ package v0.5.6 in the UK Biobank sample [53]. Mendelian randomization employs genetic instruments to test whether there is a causal effect of the exposure phenotype on the outcome phenotype. We tested two directions of causal relationship: (i) schizophrenia (exposure) causing brain NDI changes (outcome); and (ii) brain NDI changes (exposure) causing schizophrenia (outcome). We restricted MR analysis to a subset of global and regional NDI metrics that were most strongly and robustly associated with schizophrenia PRS and showed  $\geq 10$  genome-wide significant loci, to ensure reasonable statistical power (Tables S5-S6).

133 For MR analysis (i) of the causal effect of schizophrenia on NDI, we used the same GWAS summary statistics as for the PRS analyses [4]. Genetic instruments were chosen at a P threshold of  $5 \times 10^{-8}$  and clumped with a distance of 10,000 kb and LD  $r^2$  of 0.001. These SNPs were then identified within the outcome GWAS and SNP effect of exposure and outcome data were harmonised to match the effect alleles leading to 184 genetic instruments and 41 imaging phenotypes (Table S7).

137 For MR analysis (ii) of the causal effect of NDI on schizophrenia, we performed GWAS using fastGWA with sample sizes in the range  $N = 31,722 - 31,760$  for different regional metrics (SI Methods) [54]. Genetic instruments were chosen at two significance thresholds. Firstly, we used a genome-wide significant threshold of  $P = 5 \times 10^{-8}$  and clumped with a distance of 10,000 kb and LD  $r^2$  of 0.001. Based on these parameters, 40 NDI phenotypes were included and the number of genome-wide significant loci ranged from three to 29 after harmonising the data (Table S8). Secondly, we identified genetic instruments for the same 40 NDI phenotypes with a lower GWAS significance threshold of  $P = 5 \times 10^{-6}$ , as the smallest number of genetic instruments after data harmonising was three [48, 55] (Tables S5-S6). This increased the number of genetic instruments, which ranged from 21 to 71 after data harmonising (Table S9), which was expected to enhance statistical power for MR analysis at the cost of somewhat less stringent type 1 error control in construction of the instrumental variables.

146 To fit the models, we used inverse variance-weighted Mendelian randomization (IVW), which assumes that all SNPs are valid genetic instruments, as the main method to estimate causal effects [56]. The robustness of significant findings obtained using IVW was assessed using two additional methods (sensitivity analyses): weighted median method (WM), which provides consistent results even when 50% of the genetic instruments are invalid; and MR-Egger, which accounts for pleiotropy [56], and we tested for heterogeneity and horizontal pleiotropy.

151 To evaluate consistency in effect direction, we additionally calculated genetic correlations between schizophrenia and the same 41 imaging phenotypes using Linkage Disequilibrium Score Regression v1.0.1 [57] and corrected for multiple comparison using FDR.

## 154 Results

### 155 Sample

156 The sample sizes available after QC for analysis of cortical, subcortical and white matter structure varied between regions and  
 157 MRI metrics in the range  $N = 27,086-29,878$  (Fig.1). All samples comprised approximately 55% female, 45% male participants  
 158 aged 40-70 years, with mean age  $\sim 55$  years; see Tables S10 – S12 for details.

### 159 Global cortical MRI phenotypes

160 Two global cortical metrics were significantly associated with PRS at one or more  $P_{SNP}$ -value thresholds (BY = 5%). Both were  
 161 micro-structural phenotypes derived from DWI or NODDI: FA was significantly negatively associated with the PRS constructed  
 162 with  $P_{SNP} \leq 0.001$ ; and NDI was significantly negatively associated with PRS constructed at  $P_{SNP}$ 's  $\leq 0.0001, 0.001$  and  $0.01$   
 163 (Fig.2 A, Table S13). These results indicate that participants with increased polygenic risk for schizophrenia have decreased  
 164 global fractional anisotropy and neurite density index “on average” over the whole cortex. The association between PRS and  
 165 NDI was more robust to the choice of probability threshold used to construct the risk score; and PRS accounted for a larger  
 166 proportion of the variance in NDI ( $\sim 0.05\%$ ), compared to FA ( $\sim 0.02\%$ ) and other metrics.

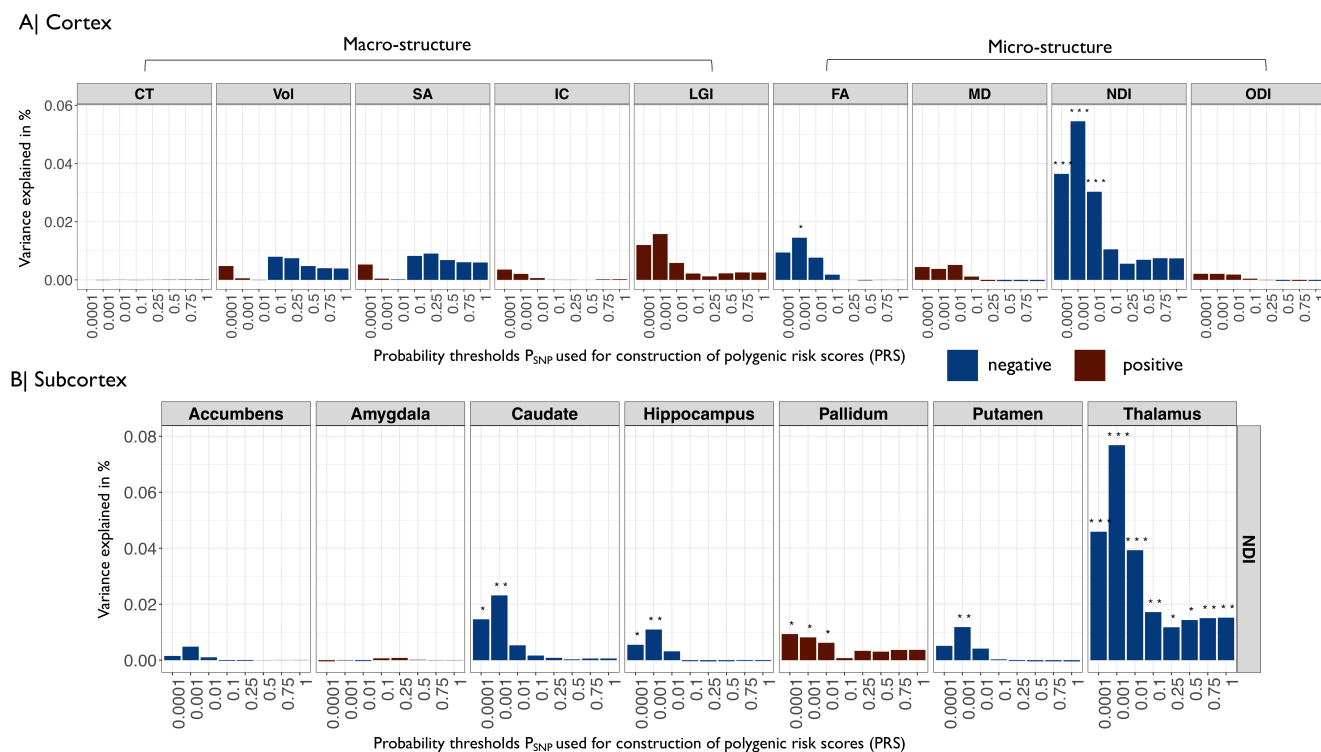


**Figure 2. Associations between polygenic risk scores for schizophrenia and global cortical (A) and regional subcortical (B) metrics of human brain structure.** (A) Barcharts of variance explained by schizophrenia PRS ( $R^2$ , y-axis) constructed at each of eight probability thresholds ( $0.0001 \geq P_{SNP} \leq 1$ , x-axis) for each of nine global mean cortical metrics: CT, cortical thickness; GMV, grey matter volume; SA surface area; IC intrinsic curvature; LGI local gyrification index; FA fractional anisotropy; MD mean diffusivity; NDI neurite density index; ODI orientation dispersion index. Blue bars indicate negative associations and red bars positive associations; asterisks indicate P-values for association after FDR correction: (\*  $P \leq 0.05$ , \*\*  $P \leq 0.01$ , \*\*\*  $P \leq 0.001$ ). Polygenic risk scores for schizophrenia were significantly negatively associated with global neurite density index and fractional anisotropy. (B) Barcharts of variance explained by PRS ( $R^2$ , y-axis) constructed at each of eight probability thresholds ( $0.0001 \geq P_{SNP} \leq 1$ , x-axis) for NDI measured at each of seven subcortical regions (colours and asterisks code sign and significance of association as in A). PRS was significantly negatively associated with NDI in thalamus, hippocampus, putamen and caudate; and significantly positively associated with NDI in pallidum.

### 167 Regional cortical MRI phenotypes

168 The macro-structural metrics (CT, SA, Vol) were positively correlated with each other and negatively correlated with LGI.  
 169 Among the micro-structural metrics, NDI and FA were positively correlated; and both were negatively correlated with MD and

170 ODI (Fig.3 A).

171 There were significant associations between PRS and eight out of nine MRI metrics in at least one cortical area, with the  
 172 exception being CT (Fig.3 B). The proportion of regional variance explained by PRS varied between metrics in the range .002%  
 173  $\leq R^2 \leq .08\%$  with  $-.03 \leq \beta \leq +.03$ ; see Table S14.

174 Among the micro-structural metrics, NDI was significantly associated with PRS in 149 cortical areas (maximum  $R^2 = .06\%$ ,  
 175  $\beta = -0.03$ ). The top ten areas where NDI was most strongly negatively associated with PRS were located in association auditory  
 176 cortex, early auditory cortex, ventral visual stream, posterior cingulate cortex, insular and frontal opercular cortex, posterior  
 177 opercular cortex, inferior parietal cortex and superior parietal cortex (see Table S15 for details). FA was negatively associated  
 178 with PRS in 63 regions (maximum  $R^2 = .01\%$ ,  $\beta = -0.01$ ); and positively associated with PRS in two regions (maximum  $R^2 =$   
 179  $.01\%$ ,  $\beta = .01$ ). The top ten regions where FA was most strongly associated with PRS were all areas of temporal, cingulate,  
 180 frontal and insular cortex, where decreased FA was associated with higher risk scores. MD was significantly associated with  
 181 PRS in 76 regions (66 positive and 10 negative associations). ODI was the micro-structural metric least frequently associated  
 182 with PRS, at 11 cortical regions.

183 Of the macro-structural metrics, LGI showed the highest number of significant associations with PRS (72 regions; 67  
 184 positive and five negative) compared to Vol, SA and IC, each of which was significant in less than 15 regions (maximum  $R^2 \leq$   
 185  $.02\%$ , maximum  $|\beta| \leq .01$ ).

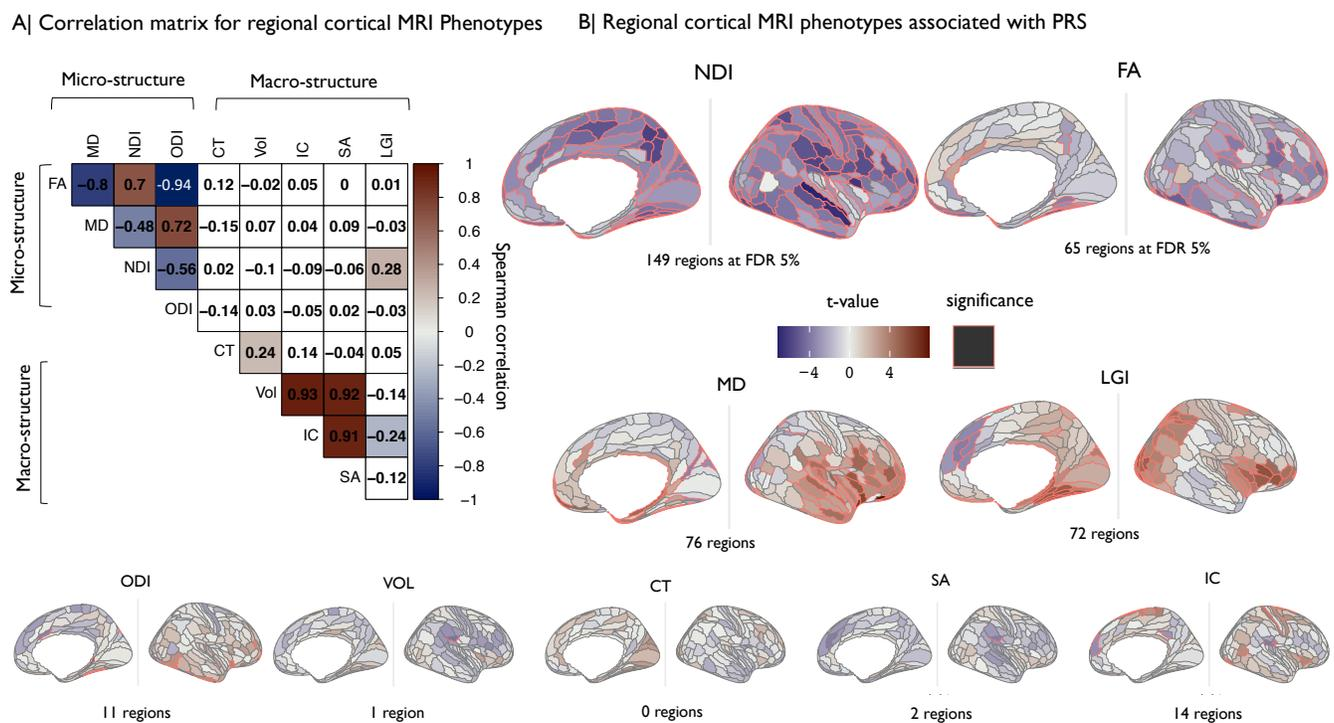


**Figure 3. Regional cortical MRI phenotypes: correlations between metrics and associations of each metric with schizophrenia polygenic risk scores.** (A) Matrix of Spearman's correlation for each pair of nine MRI metrics. Shades of blue indicate significant negative correlation and shades of red indicate significant positive correlations. (B) Cortical  $t$ -maps representing strength of association between schizophrenia PRS and regional MRI phenotypes; regions where the effect of PRS is statistically significant at FDR = 5% are outlined in red. NDI and FA metrics, which were globally decreased by genetic risk for schizophrenia (Fig.2), were significantly regionally decreased in multiple areas. MD and LGI metrics were significantly regionally increased by genetic risk in several areas.

186 Since the MRI phenotypes were not independent of each other (Fig.3 A), we further explored the spatial co-localisation of  
 187 genetic associations with different cortical metrics. The cortical  $t$ -maps of PRS association with NDI and FA were significantly  
 188 positively correlated with each other, and were negatively correlated with the cortical  $t$ -maps of PRS associations with ODI  
 189 (both NDI and FA) and MD (FA only) (Fig.4 A). In other words, regions where genetic risk was most strongly associated  
 190 with decreased FA ( $FA(t) \ll 0$ ) tended to be the same regions where PRS was most strongly associated with decreased NDI  
 191 ( $NDI(t) \ll 0$ ) and increased MD ( $MD(t) \gg 0$ ) (Fig.4 B).

192 We also simply counted the number of different MRI phenotypes that were significantly associated with PRS at each of 180

193 cortical areas. There were genetic effects on at least two metrics in 122 regions (**Table S16**), at least three metrics in 68 regions,  
194 and at least four metrics in 21 regions (**Fig.4 C**). The most frequently co-localised genetic associations were with NDI and MD  
195 (63 regions) and NDI and FA (61 regions) (see **SI Results**). Regions that were associated with PRS in terms of multiple MRI  
196 phenotypes were located in (inferior) frontal, insular, temporal, auditory and ventral visual stream areas of cortex (**Fig.4 D**,  
197 **Table S16**).

### 198 **Regional subcortical MRI phenotypes**

199 We estimated the association between PRS and one macro-structural (Vol) and four micro-structural phenotypes (MD, FA, NDI,  
200 ODI) at seven subcortical regions. The single strongest effect was a negative association between PRS and NDI of thalamus  
201 ( $R^2 = .08\%$ ,  $\beta = -.03$ ). NDI was also negatively associated with PRS in the caudate, hippocampus, and putamen; and positively  
202 associated with PRS in pallidum (**Fig.2 B**, **Table S17**). Further significant associations were found between PRS and MD of  
203 the amygdala, caudate, hippocampus, pallidum and putamen; between PRS and Vol of caudate, putamen and hippocampus;  
204 between PRS and FA of putamen and thalamus; and between PRS and ODI of pallidum and thalamus (**Figure S17**).

### 205 **Regional white matter phenotypes**

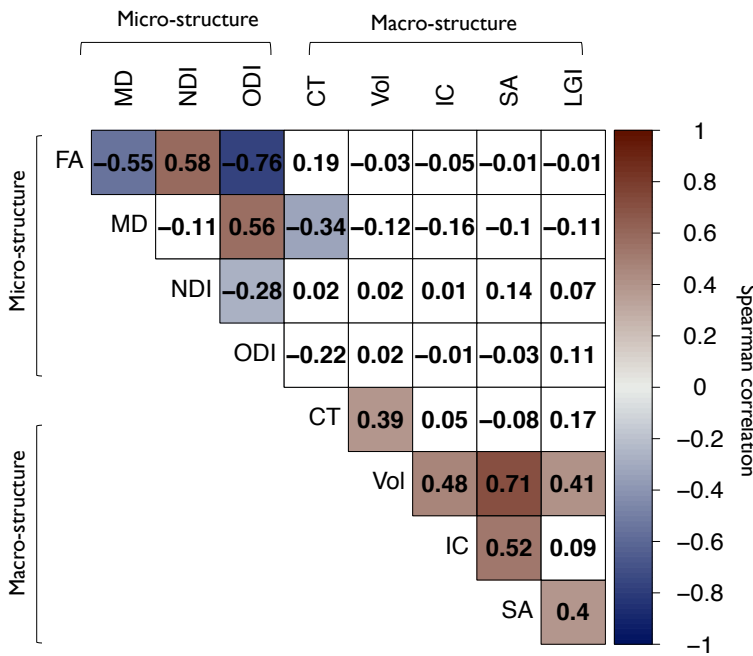
206 We identified a large number of significant associations between PRS and micro-structural metrics in 15 white matter tracts:  
207 NDI in 14 out of 15 tracts, FA in 12 tracts, MD in 11 tracts, and ODI in 5 tracts (**Fig.5**, **Fig. S19**). These results indicate  
208 that higher genetic risk for schizophrenia is associated with decreased NDI and FA, and increased MD, within callosal fibers,  
209 projection fibers, association fibers, limbic system fibers and brainstem tracts. The highest proportion of phenotypic variance  
210 explained by PRS was found for NDI of the forceps minor ( $R^2 = .12\%$ ,  $\beta = -.04$ ) followed by NDI of projection fibers (superior  
211 thalamic radiation  $R^2 = .11\%$ ,  $\beta = -.03$ ) and association fibers (inferior fronto-occipital fasciculus  $R^2 = .10\%$ ,  $\beta = -.03$ ). Those  
212 associations showed a consistent direction of effect and were significant at all  $P_{SNP}$  inclusion thresholds. The strongest negative  
213 association between PRS and FA was within the forceps minor ( $R^2 = .11\%$ ,  $\beta = -.03$ ), followed by projection fibers (superior  
214 thalamic radiation  $R^2 = .06\%$ ,  $\beta = -.02$ ), and association fibers (anterior thalamic radiation  $R^2 = .06\%$ ,  $\beta = -.02$ ). The strongest  
215 positive associations between PRS and MD were located in association fibers (uncinate fasciculus  $R^2 = .07\%$ ,  $\beta = .03$ ) followed  
216 by limbic system fibers (cingulate gyrus part of cingulum  $R^2 = .04\%$ ,  $\beta = .02$ ) and the forceps minor ( $R^2 = .03\%$ ,  $\beta = .02$ )  
217 (**Table S18**).

### 218 **Bidirectional Mendelian randomization on schizophrenia and NDI metrics**

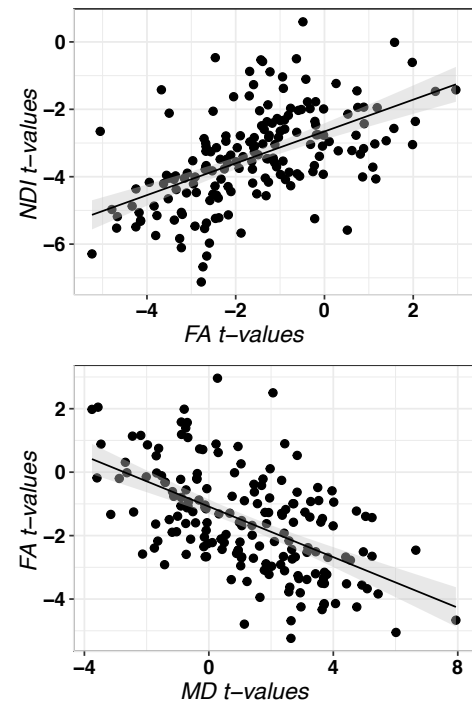
219 For these post-hoc analyses of causality, we focused on 41 NDI phenotypes (global NDI and regional NDI metrics in 21  
220 cortical areas, 5 subcortical nuclei, and 14 white matter tracts). After correction for multiple comparisons, there was no  
221 significant evidence for a causal effect of schizophrenia on NDI metrics (MR (i)), and there was no significant evidence for  
222 a causal effect of NDI metrics on schizophrenia (MR (ii)) using genetic instruments identified by genome-wide association  
223 significance threshold of  $P = 5 \times 10^{-8}$  (**Tables S7, S8**). However, for MR (ii), when we relaxed the inclusion threshold for  
224 genetic instruments to  $P = 5 \times 10^{-6}$ , we found that lower genetically predicted NDI in the thalamus was associated with  
225 increased genetically predicted risk for schizophrenia (IVW method  $\beta = -0.16$ ,  $P_{FDR} = 0.02$ ), suggesting that reduced thalamic  
226 NDI may cause increased risk of schizophrenia. Sensitivity analyses using the weighted median method were also significant  
227 ( $\beta = -0.14$ ,  $P = 0.002$ ). NDI of thalamus showed significant heterogeneity between individual genetic variants ( $P$  for Q-test <  
228 0.0001) but the Egger intercept was not significant, suggesting no evidence for substantial pleiotropic effects ( $P = 0.42$ ) (**Table**  
229 **S9**). Additionally, leave-one-out analysis did not indicate that the result was driven by any one genetic variant (**Figure S20**).

230 Genetic correlations were modest and did not survive multiple testing correction. However, 80% of the correlations were in  
231 the negative direction predicted by significant negative associations between NDI and PRS scores (**Table S19**).

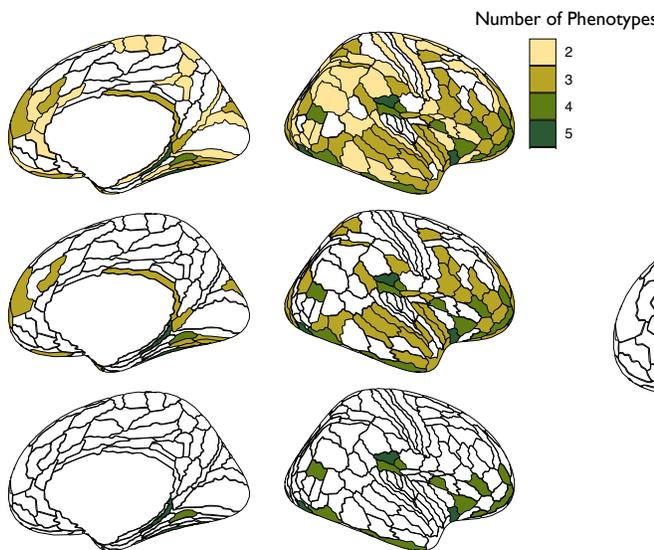
### A| T- map spatial correlation



### B| Scatterplot



### C| Regions implicated by multiple phenotypes



### D| Annotated regions

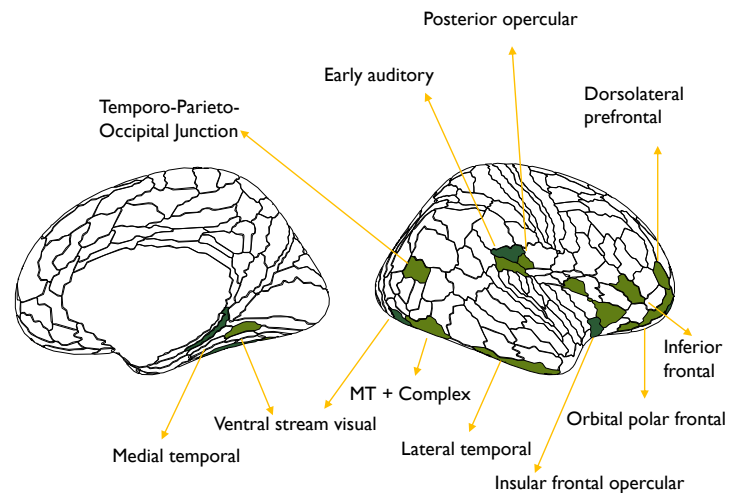


**Figure 4. Anatomical co-localisation of polygenic risk effects for schizophrenia on multiple MRI phenotypes.** (A) Matrix of spatial correlations between cortical *t*-maps of association between schizophrenia PRS and nine MRI metrics. (B) Scatterplot showing the relationships between (top) cortical *t*-maps of FA and NDI and (bottom) cortical *t*-maps of FA and MD; each point represents a cortical area. (C) Cortical map colour coded to indicate the number of MRI phenotypes that were significantly associated with schizophrenia PRS at each region. Coloured regions had at least two (top), three (middle), or four (bottom), MRI phenotypes significantly associated with genetic risk of schizophrenia. (D) The brain regions where schizophrenia PRS was significantly associated with four MRI phenotypes were anatomically located in medial and lateral temporal cortex, ventral visual stream, insular and frontal cortex.

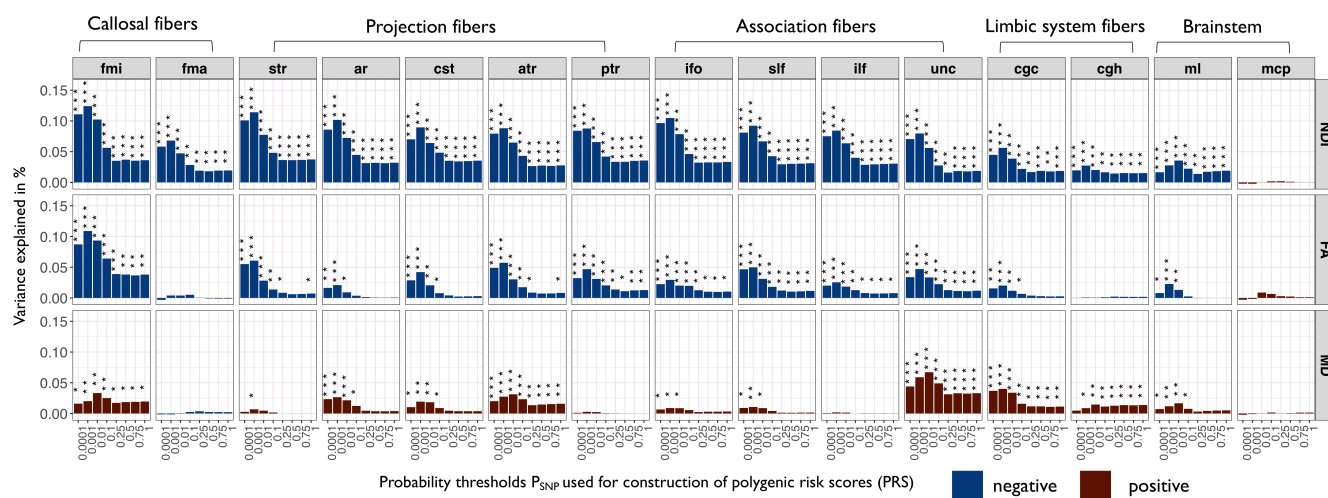


**Figure 5. Associations between polygenic risk scores for schizophrenia and white matter tracts.** Barcharts of variance explained by schizophrenia PRS ( $R^2$ , y-axis) constructed at each of eight probability thresholds ( $0.0001 \geq P_{SNP} \leq 1$ , x-axis) for each of three white matter metrics (NDI neurite density index; FA fractional anisotropy; MD mean diffusivity) measured at 15 major white matter tracts: mcp, middle cerebellar peduncle; ml, medial lemniscus; cst, corticospinal tract; ar, acoustic radiation; atr, anterior thalamic radiation; str, superior thalamic radiation; pts, posterior thalamic radiation; slf, superior longitudinal fasciculus; ilf, inferior longitudinal fasciculus; ifo, inferior fronto-occipital fasciculus; unc, uncinate fasciculus; cgc, cingulate gyrus part of cingulum; cgh, parahippocampal part of cingulum; fmi, forceps minor; and fma, forceps major. Blue bars indicate negative associations and red bars positive associations; asterisks indicate P-values for association after FDR correction: \*  $P \leq 0.05$ , \*\*  $P \leq 0.01$ , \*\*\*  $P \leq 0.001$ . Polygenic risk scores for schizophrenia were significantly associated with NDI, FA and MD of multiple white matter tracts.

## 232 Discussion

233 We estimated the strength of association between polygenic risk scores for schizophrenia and nine MRI phenotypes measured  
234 at 180 cortical areas, seven subcortical structures and 15 white matter tracts. In strong support of our motivating hypothesis, we  
235 found that PRS was significantly associated with micro-structural metrics of brain tissue composition at global and regional  
236 scales of cortex; in the thalamus, basal ganglia and hippocampus; and extensively in white matter tracts. First we interpret and  
237 integrate these signals of significant association between genetic risk for schizophrenia and brain MRI metrics, especially NDI;  
238 then we discuss post-hoc analyses of causality stimulated by these results.

### 239 **Neurite density index - a plausible brain MRI marker for schizophrenia risk?**

240 Of all nine MRI metrics considered, NDI was the most robustly associated with PRS. NDI is derived from NODDI, an MRI  
241 sequence that was developed to estimate the micro-structural complexity of dendrites and axons - collectively referred to as  
242 neurites - in grey and white matter of the living brain. NODDI compartmentalizes tissue into three microstructural environments  
243 - intra-cellular, extra-cellular, and cerebro-spinal fluid - each of which has different diffusion properties. The intra-cellular  
244 compartment refers to the space bound by neurites and allows for the measurement of their density (NDI) and their spatial  
245 orientation (ODI) [58, 59]. *In vivo* estimates of NDI have been biologically validated by *ex vivo*, histological estimates of  
246 neurite density in mice [60], and correlated with cortical myelination in humans [59].

247 Thus, a reasonable interpretation of our results is that polygenic risk for schizophrenia in the general population is associated  
248 with decreased axonal and/or dendritic density in grey and white matter. While we cannot ascribe causality using the current  
249 methods, this interpretation is consistent with several lines of previous research in individuals with schizophrenia. First,  
250 schizophrenia case-control studies have reported abnormally decreased NDI in the cortex, hippocampus and white matter  
251 [26, 35]. Secondly, post-mortem studies have reported multiple abnormalities of neurite structure in schizophrenia, including  
252 reduced dendritic arborisation [61], reduced spine density [61], reduced axonal myelination [62], and reduced oligodendrocytes  
253 [63]. Third, recent GWAS studies have identified risk genes for schizophrenia that are expressed in neurons and implicated  
254 in dendritic arborization and microcircuit formation, synaptic plasticity, and glutamatergic neurotransmission [4, 64, 65]. It  
255 is intriguing to speculate which individual risk genes might be most relevant to the relationship between PRS and reduced  
256 NDI but we cannot certainly resolve this question from these results. Fourth, locally reduced density of myelinated axons and  
257 dendrites will likely reflect atypical connectivity between brain structures [62, 66], as anticipated by long-standing theories of  
258 schizophrenia as a dysconnectivity syndrome [67, 68, 69, 70].

### 259 **Integration of genetic effects across cortical phenotypes**

260 While NDI was the one most strongly associated with PRS, almost all other metrics (except CT) also showed some significant  
261 regional associations with genetic risk. We consider that this apparent pleiotropy of genetic effects on brain structure largely  
262 reflects correlations between the MRI metrics [27]. For example, NDI was positively correlated with FA, and both NDI and FA  
263 were negatively correlated with MD (Fig. 3). This is not surprising because increased NDI restricts isotropic diffusion of protons  
264 in the tissue water compartment so that FA is increased and MD is decreased [27]. These three metrics are thus complementary  
265 measures of the same or similar tissue composition characteristics, which explains the anatomical co-localisation of genetic  
266 effects on NDI, FA and MD (Fig. 4). These co-localised, multi-metric associations with PRS were concentrated in auditory  
267 and lateral temporal cortex, pre-frontal and orbito-frontal cortex, anterior cingulate cortex, and insular cortical areas, many  
268 of which have previously been reported to show increased MD and/or decreased FA in case-control studies of schizophrenia  
269 [28, 29, 30, 31].

270 Of the macro-structural phenotypes, LGI was positively correlated with MD and positively associated with genetic risk  
271 for schizophrenia. Local gyrification is assumed to capture early neurodevelopmental changes that are relatively stable after  
272 birth [25, 71]. Case-control data have recently shown increased LGI in schizophrenia, interpreted as a marker of structural  
273 dysconnectivity [25]. It is uncertain whether polygenic effects on macro-structural markers are mechanistically distinct from  
274 the effects on NDI and related micro-structural markers. However, micro-structural MRI metrics were clearly more strongly  
275 associated with genetic risk for schizophrenia than the macro-structural metrics that have previously been investigated as  
276 candidate endophenotypes.

### 277 **Genetic risk and subcortical structures**

278 Atypicality in subcortical structures is a frequently reported finding in schizophrenia cases [12], and in their non-psychotic  
279 first-degree relatives [72], compared to healthy controls. However, this is the first study to identify significant associations  
280 between polygenic risk for schizophrenia and subcortical structures in a population sample.

281 NDI was again the MRI metric most sensitive to genetic association, especially in the thalamus, where PRS was significantly  
282 associated with reduced NDI. The thalamus plays a key role in cognitive and emotional processes that are clinically impaired in  
283 schizophrenia [73, 74]. Thalamic volume reductions [73] and abnormal functional connectivity between thalamus and cortex

284 [75] have been previously reported in schizophrenia. The basal ganglia (putamen, pallidum and caudate nucleus) and the  
285 hippocampus also demonstrated PRS-related changes in NDI and related micro-structural metrics. There was also a robust  
286 (negative) association between PRS and hippocampal volume, consistent with extensively replicated case-control differences in  
287 hippocampal volume [12].

### 288 **Genetic risk and white matter tracts**

289 Abnormalities of white matter micro-structure, consistent with aberrant inter-hemispheric, fronto-temporal and cortico-thalamic  
290 connectivity, have been frequently reported in schizophrenia [14, 33]. We identified significant associations between genetic  
291 risk for schizophrenia and micro-structural metrics in most of the major axonal tracts we measured, indicating that PRS is  
292 associated with widespread disruption or disorganization of white matter. The strongest effect was a negative association  
293 between PRS and NDI of the forceps minor, the anterior part of the corpus callosum, inter-hemispherically connecting the  
294 frontal lobes. However, PRS was also significantly associated with NDI, FA and MD in intra-hemispheric association fibers,  
295 cortico-subcortical projection fibers, limbic system and brainstem fibers, indicating that genetic risk for schizophrenia is  
296 associated with anatomically widespread disruption of white matter tracts.

### 297 **Investigation of causality**

298 Association between PRS and brain MRI metrics, however statistically significant or anatomically plausible, is uninformative  
299 about the underlying direction of causality. In post-hoc analyses restricted to a subset of the NDI metrics most strongly  
300 associated with schizophrenia, we used bidirectional Mendelian randomization to test for causal effects of schizophrenia  
301 on NDI metrics (MR(i)), and for causal effects of NDI metrics on schizophrenia (MR(ii)). We found no evidence for a  
302 significant causal effect of schizophrenia on global grey matter, cortical, subcortical or white matter tract NDI metrics. We also  
303 did not find significant causal effects of any NDI metrics on schizophrenia using genetic instruments selected at a stringent  
304 GWAS-significant threshold of  $P = 5 \times 10^{-8}$ . However, we did find a significant, potentially causal relationship between lower  
305 NDI in the thalamus and increased risk for schizophrenia when we used a less stringent significance threshold to increase the  
306 number of genetic instruments and thus boost the power of MR analysis. We consider that this amounts to suggestive evidence  
307 that thalamic NDI may causally predict schizophrenia, consistent with the prior observation that thalamic NDI was the regional  
308 MRI metric most strongly and robustly associated with PRS for schizophrenia. However, we also consider that the sample  
309 size available for GWAS of NDI metrics was under-powered to identify sufficient instrumental variables at the conventional  
310 threshold for genome-wide significance (or to estimate genome-wide associations with sufficient efficiency for significant  
311 genetic correlation analysis). More definitive investigations of the causal relationship between MRI metrics and schizophrenia,  
312 on the basis of better genetic instruments defined by larger MRI samples, will be important to pursue in future [48].

### 313 **Strengths and limitations**

314 It is a strength that we used the largest GWAS to date to construct schizophrenia PRS at multiple  $P_{SNP}$ -value thresholds for  
315 inclusion of risk variants. We also used the largest and most methodologically diverse MRI dataset to date in order to assess  
316 PRS associations with brain structure. However, the diagnostic variance in schizophrenia explained by PRS is still relatively  
317 small (7.7%) [4] and, in line with previous findings [6, 19], the proportion of variance in cortical and subcortical structures  
318 explained by the PRS is even smaller ( $< 1\%$ ). It is expected that even larger sample sizes in future studies might implicate  
319 other brain structures or MRI metrics than those significantly associated with PRS in this study [4]. The reported results should  
320 be more robustly assessed by future translational MRI and histological studies of grey and white matter micro-structure in  
321 human post mortem data or animal models of genetic risk for schizophrenia. Finally, the UK Biobank is an ageing cohort of  
322 largely European descent that is on average wealthier and healthier than the general population [76]. The generalisability of  
323 these results should be investigated in more demographically diverse and epidemiologically relevant samples.

### 324 **Summary**

325 Polygenic risk scores for schizophrenia were most robustly associated with significant changes in micro-structural MRI metrics  
326 in the cortex, the subcortex, and white matter tracts, in a large population sample. These results provide substantial new  
327 evidence in support of the pathogenic model that genetic risk for schizophrenia is associated with reduced neurite density, and  
328 anatomical dysconnectivity, in cortico-subcortical networks.

## 329 Acknowledgements

330 E.-M.S. is supported by a PhD studentship awarded by the Friends of Peterhouse. This research was co-funded by the National  
331 Institute of Health Research (NIHR) Cambridge Biomedical Research Centre and a Marmaduke Sheild grant to R.A.I.B. and  
332 V.W. E.T.B. is an NIHR Senior Investigator. R.R.G was funded by a Guarantors of Brain Fellowship. R.A.I.B. is supported by  
333 a British Academy Post-Doctoral fellowship and the Autism Research Trust. We wish to thank Dr Petra Vertes and Dr Lisa  
334 Ronan for their advice on research design and Dr Simon R White for his statistical advice and support. The views expressed  
335 are those of the author(s) and not necessarily those of the NHS, the NIHR or the Department of Health and Social Care. This  
336 research was possible due to an application to the UK Biobank (project 20904).

## 337 Author contributions statement

338 E.-M.S., R.A.I.B., V.W., G.K.M. and E.T.B. designed research. J.S. advised on research design. E.-M.S., R.A.I.B., V.W., and  
339 R.R.G. analyzed data. E.-M.S. and R.A.I.B. made figures. E.-M.S., R.A.I.B. and V.W. performed research. E.-M.S. and E.T.B.  
340 wrote the paper.

## 341 Disclosures/Competing Interests statement

342 E.T.B. serves on the Scientific Advisory Board of Sosei Heptares and as a consultant for GlaxoSmithKline. All other authors  
343 declare no conflicts of interest.

## 344 References

- 345 1. Hilker, R. *et al.* Heritability of schizophrenia and schizophrenia spectrum based on the nationwide danish twin register.  
346 *Biol. psychiatry* **83**, 492–498 (2018).
- 347 2. Sullivan, P. F., Kendler, K. S. & Neale, M. C. Schizophrenia as a complex trait: evidence from a meta-analysis of twin  
348 studies. *Arch. general psychiatry* **60**, 1187–1192 (2003).
- 349 3. Pardiñas, A. F. *et al.* Common schizophrenia alleles are enriched in mutation-intolerant genes and in regions under strong  
350 background selection. *Nat. genetics* **50**, 381–389 (2018).
- 351 4. Ripke, S., Walters, J. T., O’Donovan, M. C., of the Psychiatric Genomics Consortium, S. W. G. *et al.* Mapping genomic  
352 loci prioritises genes and implicates synaptic biology in schizophrenia. *medRxiv* (2020).
- 353 5. Riglin, L. *et al.* Schizophrenia risk alleles and neurodevelopmental outcomes in childhood: a population-based cohort  
354 study. *The Lancet Psychiatry* **4**, 57–62 (2017).
- 355 6. Neilson, E. *et al.* Impact of polygenic risk for schizophrenia on cortical structure in uk biobank. *Biol. psychiatry* **86**,  
356 536–544 (2019).
- 357 7. Smeland, O. B., Frei, O., Dale, A. M. & Andreassen, O. A. The polygenic architecture of schizophrenia—rethinking  
358 pathogenesis and nosology. *Nat. Rev. Neurol.* 1–14 (2020).
- 359 8. Gottesman, I. I. & Gould, T. D. The endophenotype concept in psychiatry: etymology and strategic intentions. *Am. journal*  
360 *psychiatry* **160**, 636–645 (2003).
- 361 9. Fornito, A. & Bullmore, E. T. Connectomic intermediate phenotypes for psychiatric disorders. *Front. psychiatry* **3**, 32  
362 (2012).
- 363 10. Bigos, K. L. & Weinberger, D. R. Imaging genetics—days of future past. *Neuroimage* **53**, 804–809 (2010).
- 364 11. Bogdan, R. *et al.* Imaging genetics and genomics in psychiatry: a critical review of progress and potential. *Biol. psychiatry*  
365 **82**, 165–175 (2017).
- 366 12. van Erp, T. G. *et al.* Subcortical brain volume abnormalities in 2028 individuals with schizophrenia and 2540 healthy  
367 controls via the enigma consortium. *Mol. psychiatry* **21**, 547–553 (2016).
- 368 13. Van Erp, T. G. *et al.* Cortical brain abnormalities in 4474 individuals with schizophrenia and 5098 control subjects via the  
369 enhancing neuro imaging genetics through meta analysis (enigma) consortium. *Biol. psychiatry* **84**, 644–654 (2018).

- 370 **14.** Kelly, S. *et al.* Widespread white matter microstructural differences in schizophrenia across 4322 individuals: results from  
371 the enigma schizophrenia dti working group. *Mol. psychiatry* **23**, 1261–1269 (2018).
- 372 **15.** Satizabal, C. L. *et al.* Genetic architecture of subcortical brain structures in 38,851 individuals. *Nat. genetics* **51**, 1624–1636  
373 (2019).
- 374 **16.** Grasby, K. L. *et al.* The genetic architecture of the human cerebral cortex. *Science* **367** (2020).
- 375 **17.** Kochunov, P. *et al.* Heritability of fractional anisotropy in human white matter: a comparison of human connectome project  
376 and enigma-dti data. *Neuroimage* **111**, 300–311 (2015).
- 377 **18.** van der Merwe, C. *et al.* Polygenic risk for schizophrenia and associated brain structural changes: A systematic review.  
378 *Compr. psychiatry* **88**, 77–82 (2019).
- 379 **19.** Reus, L. M. *et al.* Association of polygenic risk for major psychiatric illness with subcortical volumes and white matter  
380 integrity in uk biobank. *Sci. reports* **7**, 42140 (2017).
- 381 **20.** Franke, B. *et al.* Genetic influences on schizophrenia and subcortical brain volumes: large-scale proof of concept. *Nat.*  
382 *neuroscience* **19**, 420–431 (2016).
- 383 **21.** Grama, S. *et al.* Polygenic risk for schizophrenia and subcortical brain anatomy in the uk biobank cohort. *Transl. psychiatry*  
384 **10**, 1–10 (2020).
- 385 **22.** Van Scheltinga, A. F. T. *et al.* Genetic schizophrenia risk variants jointly modulate total brain and white matter volume.  
386 *Biol. psychiatry* **73**, 525–531 (2013).
- 387 **23.** Ellison-Wright, I. & Bullmore, E. Anatomy of bipolar disorder and schizophrenia: a meta-analysis. *Schizophr. research*  
388 **117**, 1–12 (2010).
- 389 **24.** Ronan, L. *et al.* Consistency and interpretation of changes in millimeter-scale cortical intrinsic curvature across three  
390 independent datasets in schizophrenia. *Neuroimage* **63**, 611–621 (2012).
- 391 **25.** Sasabayashi, D. *et al.* Increased brain gyrification in the schizophrenia spectrum. *Psychiatry Clin. Neurosci.* **74**, 70–76  
392 (2020).
- 393 **26.** Nazeri, A. *et al.* Gray matter neuritic microstructure deficits in schizophrenia and bipolar disorder. *Biol. psychiatry* **82**,  
394 726–736 (2017).
- 395 **27.** Fukutomi, H. *et al.* Diffusion tensor model links to neurite orientation dispersion and density imaging at high b-value in  
396 cerebral cortical gray matter. *Sci. reports* **9**, 1–12 (2019).
- 397 **28.** McKenna, F. F., Miles, L., Babb, J. S., Goff, D. C. & Lazar, M. Diffusion kurtosis imaging of gray matter in schizophrenia.  
398 *Cortex* **121**, 201–224 (2019).
- 399 **29.** Narr, K. L. *et al.* Mean diffusivity: a biomarker for csf-related disease and genetic liability effects in schizophrenia.  
400 *Psychiatry Res. Neuroimaging* **171**, 20–32 (2009).
- 401 **30.** Spoletini, I. *et al.* Hippocampi, thalami, and accumbens microstructural damage in schizophrenia: a volumetry, diffusivity,  
402 and neuropsychological study. *Schizophr. bulletin* **37**, 118–130 (2011).
- 403 **31.** Kalus, P. *et al.* New evidence for involvement of the entorhinal region in schizophrenia: a combined mri volumetric and dti  
404 study. *Neuroimage* **24**, 1122–1129 (2005).
- 405 **32.** Woodward, N. & Parvatheni, P. M82. neurite orientation dispersion and density imaging (noddi) of the prefrontal cortex in  
406 psychosis. *Schizophr. Bull.* **43**, S240 (2017).
- 407 **33.** Ellison-Wright, I. & Bullmore, E. Meta-analysis of diffusion tensor imaging studies in schizophrenia. *Schizophr. research*  
408 **108**, 3–10 (2009).
- 409 **34.** Kraguljac, N. V. *et al.* Neurite orientation dispersion and density imaging (noddi) and duration of untreated psychosis in  
410 antipsychotic medication-naïve first episode psychosis patients. *Neuroimage: Reports* **1**, 100005 (2021).

- 411 **35.** Rae, C. L. *et al.* Deficits in neurite density underlie white matter structure abnormalities in first-episode psychosis. *Biol.*  
412 *psychiatry* **82**, 716–725 (2017).
- 413 **36.** Choi, S. W. & O’Reilly, P. F. Prsice-2: Polygenic risk score software for biobank-scale data. *Gigascience* **8**, giz082 (2019).
- 414 **37.** Ripke, S. *et al.* Biological insights from 108 schizophrenia-associated genetic loci. *Nature* **511**, 421–427 (2014).
- 415 **38.** Sudlow, C. *et al.* Uk biobank: an open access resource for identifying the causes of a wide range of complex diseases of  
416 middle and old age. *PLoS medicine* **12** (2015).
- 417 **39.** Alfaro-Almagro, F. *et al.* Image processing and quality control for the first 10,000 brain imaging datasets from uk biobank.  
418 *Neuroimage* **166**, 400–424 (2018).
- 419 **40.** Fischl, B. *et al.* Automatically Parcellating the Human Cerebral Cortex. *Cereb. Cortex* **14**, 11–22, DOI: [10.1093/cercor/](https://doi.org/10.1093/cercor/bhg087)  
420 [bhg087](https://doi.org/10.1093/cercor/bhg087) (2004). <https://academic.oup.com/cercor/article-pdf/14/1/11/1193353/bhg087.pdf>.
- 421 **41.** Glasser, M. F. *et al.* A multi-modal parcellation of human cerebral cortex. *Nature* **536**, 171–178 (2016).
- 422 **42.** Daducci, A. *et al.* Accelerated microstructure imaging via convex optimization (amico) from diffusion mri data. *NeuroImage*  
423 **105**, 32–44 (2015).
- 424 **43.** De Groot, M. *et al.* Improving alignment in tract-based spatial statistics: evaluation and optimization of image registration.  
425 *Neuroimage* **76**, 400–411 (2013).
- 426 **44.** Bycroft, C. *et al.* The uk biobank resource with deep phenotyping and genomic data. *Nature* **562**, 203–209 (2018).
- 427 **45.** Yang, J., Lee, S. H., Goddard, M. E. & Visscher, P. M. Gcta: a tool for genome-wide complex trait analysis. *The Am. J.*  
428 *Hum. Genet.* **88**, 76–82 (2011).
- 429 **46.** Martin, A. R., Daly, M. J., Robinson, E. B., Hyman, S. E. & Neale, B. M. Predicting polygenic risk of psychiatric disorders.  
430 *Biol. psychiatry* **86**, 97–109 (2019).
- 431 **47.** Warrier, V. & Baron-Cohen, S. Childhood trauma, life-time self-harm, and suicidal behaviour and ideation are associated  
432 with polygenic scores for autism. *Mol. psychiatry* 1–15 (2019).
- 433 **48.** Shen, X. *et al.* A phenome-wide association and mendelian randomisation study of polygenic risk for depression in uk  
434 biobank. *Nat. communications* **11**, 1–16 (2020).
- 435 **49.** Privé, F., Vilhjálmsón, B. J., Aschard, H. & Blum, M. G. Making the most of clumping and thresholding for polygenic  
436 scores. *The Am. J. Hum. Genet.* **105**, 1213–1221 (2019).
- 437 **50.** R Core Team. *R: A Language and Environment for Statistical Computing*. R Foundation for Statistical Computing, Vienna,  
438 Austria (2018).
- 439 **51.** Smith, S. M. & Nichols, T. E. Statistical challenges in “big data” human neuroimaging. *Neuron* **97**, 263–268 (2018).
- 440 **52.** Shen, X. *et al.* Subcortical volume and white matter integrity abnormalities in major depressive disorder: findings from uk  
441 biobank imaging data. *Sci. reports* **7**, 1–10 (2017).
- 442 **53.** Hemani, G. *et al.* The mr-base platform supports systematic causal inference across the human phenome. *elife* **7**, e34408  
443 (2018).
- 444 **54.** Jiang, L. *et al.* A resource-efficient tool for mixed model association analysis of large-scale data. *Nat. genetics* **51**,  
445 1749–1755 (2019).
- 446 **55.** Gage, S. H. *et al.* Assessing causality in associations between cannabis use and schizophrenia risk: a two-sample mendelian  
447 randomization study. *Psychol. medicine* **47**, 971–980 (2017).
- 448 **56.** Bowden, J., Davey Smith, G., Haycock, P. C. & Burgess, S. Consistent estimation in mendelian randomization with some  
449 invalid instruments using a weighted median estimator. *Genet. epidemiology* **40**, 304–314 (2016).
- 450 **57.** Bulik-Sullivan, B. *et al.* An atlas of genetic correlations across human diseases and traits. *Nat. genetics* **47**, 1236–1241  
451 (2015).

- 452 **58.** Zhang, H., Schneider, T., Wheeler-Kingshott, C. A. & Alexander, D. C. Noddi: practical in vivo neurite orientation  
453 dispersion and density imaging of the human brain. *Neuroimage* **61**, 1000–1016 (2012).
- 454 **59.** Fukutomi, H. *et al.* Neurite imaging reveals microstructural variations in human cerebral cortical gray matter. *Neuroimage*  
455 **182**, 488–499 (2018).
- 456 **60.** Gong, N.-J., Dibb, R., Pletnikov, M., Benner, E. & Liu, C. Imaging microstructure with diffusion and susceptibility mr:  
457 neuronal density correlation in disrupted-in-schizophrenia-1 mutant mice. *NMR biomedicine* **33**, e4365 (2020).
- 458 **61.** Moyer, C. E., Shelton, M. A. & Sweet, R. A. Dendritic spine alterations in schizophrenia. *Neurosci. letters* **601**, 46–53  
459 (2015).
- 460 **62.** Flynn, S. *et al.* Abnormalities of myelination in schizophrenia detected in vivo with mri, and post-mortem with analysis of  
461 oligodendrocyte proteins. *Mol. psychiatry* **8**, 811–820 (2003).
- 462 **63.** Raabe, F. J. *et al.* Oligodendrocytes as a new therapeutic target in schizophrenia: from histopathological findings to  
463 neuron-oligodendrocyte interaction. *Cells* **8**, 1496 (2019).
- 464 **64.** Sekar, A. *et al.* Schizophrenia risk from complex variation of complement component 4. *Nature* **530**, 177–183 (2016).
- 465 **65.** Harrison, P. J. & Weinberger, D. R. Schizophrenia genes, gene expression, and neuropathology: on the matter of their  
466 convergence. *Mol. psychiatry* **10**, 40–68 (2005).
- 467 **66.** Alexander-Bloch, A. F. *et al.* Abnormal cortical growth in schizophrenia targets normative modules of synchronized  
468 development. *Biol. psychiatry* **76**, 438–446 (2014).
- 469 **67.** Morgan, S. E. *et al.* Cortical patterning of abnormal morphometric similarity in psychosis is associated with brain  
470 expression of schizophrenia-related genes. *Proc. Natl. Acad. Sci.* **116**, 9604–9609 (2019).
- 471 **68.** Nelson, B. G., Bassett, D. S., Camchong, J., Bullmore, E. T. & Lim, K. O. Comparison of large-scale human brain  
472 functional and anatomical networks in schizophrenia. *NeuroImage: Clin.* **15**, 439–448 (2017).
- 473 **69.** Schmitt, A., Hasan, A., Gruber, O. & Falkai, P. Schizophrenia as a disorder of disconnectivity. *Eur. archives psychiatry*  
474 *clinical neuroscience* **261**, 150 (2011).
- 475 **70.** Friston, K. J. & Frith, C. D. Schizophrenia: a disconnection syndrome. *Clin Neurosci* **3**, 89–97 (1995).
- 476 **71.** Zilles, K., Palomero-Gallagher, N. & Amunts, K. Development of cortical folding during evolution and ontogeny. *Trends*  
477 *neurosciences* **36**, 275–284 (2013).
- 478 **72.** McIntosh, A. M. *et al.* Voxel-based morphometry of patients with schizophrenia or bipolar disorder and their unaffected  
479 relatives. *Biol. psychiatry* **56**, 544–552 (2004).
- 480 **73.** Pergola, G., Selvaggi, P., Trizio, S., Bertolino, A. & Blasi, G. The role of the thalamus in schizophrenia from a neuroimaging  
481 perspective. *Neurosci. & Biobehav. Rev.* **54**, 57–75 (2015).
- 482 **74.** Wagner, G. *et al.* Structural basis of the fronto-thalamic dysconnectivity in schizophrenia: a combined dcm-vbm study.  
483 *NeuroImage: Clin.* **3**, 95–105 (2013).
- 484 **75.** Chen, P., Ye, E., Jin, X., Zhu, Y. & Wang, L. Association between thalamocortical functional connectivity abnormalities  
485 and cognitive deficits in schizophrenia. *Sci. reports* **9**, 1–10 (2019).
- 486 **76.** Fry, A. *et al.* Comparison of sociodemographic and health-related characteristics of uk biobank participants with those of  
487 the general population. *Am. journal epidemiology* **186**, 1026–1034 (2017).  
488 main